LETTERS

Resonant slow fault slip in subduction zones forced by climatic load stress

Anthony R. Lowry[1]†

Global Positioning System (GPS) measurements at subduction plate boundaries often record fault movements similar to earthquakes but much slower, occurring over timescales of ~1 week to ~1 year. These 'slow slip events' have been observed in Japan[1,2], Cascadia[3–7], Mexico[8,9], Alaska[10] and New Zealand[11]. The phenomenon is poorly understood, but several observations hint at the processes underlying slow slip. Although slip itself is silent, seismic instruments often record coincident low-amplitude tremor in a narrow (1–5 cycles per second) frequency range[12]. Also, modelling of GPS data[3,7,9] and estimates of tremor location[13] indicate that slip focuses near the transition from unstable ('stick-slip') to stable friction at the deep limit of the earthquake-producing seismogenic zone. Perhaps most intriguingly, slow slip is periodic at several locations, with recurrence varying from 6 to 18 months depending on which subduction zone (or even segment) is examined[4–6,9]. Here I show that such periodic slow fault slip may be a resonant response to climate-driven stress perturbations. Fault slip resonance helps to explain why slip events are periodic, why periods differ from place to place and why slip focuses near the base of the seismogenic zone. Resonant slip should initiate within the rupture zone of future great earthquakes, suggesting that slow slip may illuminate fault properties that control earthquake slip.

Observations of slow slip behaviour and associated tremor have spurred inquiry into several possible mechanisms. Seismic observations of harmonic tremor suggest a role for fluid flux, as similar volcanic tremor results from flux-driven resonance of fluid-filled cracks[14]. Coincidence of tremor and slip has prompted the inference that de-watering of subducted oceanic lithosphere reduces effective normal stress and lubricates slow slip[15]. However, tremor source locations are distributed throughout the upper plate, suggesting instead that tremor is triggered by stress/strain during slip[13].

Focusing of slip near the base of the seismogenic zone indicates a role for frictional dynamics. GPS data are ambiguous about deformation sources because the signal-to-noise ratios are low; data from the Cocos–North America plate boundary (Fig. 1) are fitted about equally well by models that locate slip partly within the zone of interplate earthquake rupture and by models that place slip entirely downdip[9] (Fig. 1 inset). Tremor source locations are less uncertain, and Cascadia sources occupy a narrow horizontal band[13] that approximately overlies the frictional transition from seismogenic velocity-weakening ('stick-slip') to velocity-strengthening ('stable')[16]. Numerical models of rate- and state-dependent frictional slip provide independent support for this interpretation. Models specifying a Ruina–Dieterich constitutive law for frictional slip produce slow slip events near the base of the seismogenic zone[17,18]. However, frequency and propagation characteristics of these simulated events are quite different from those observed in the Earth.

Slow slip in the Puget basin of Cascadia recurs at intervals of 14.7 ± 1.2 months (refs 4, 7), and predictions of event timing have been reliable enough for experiments to be designed around them. This quasi-periodicity prompted Shen *et al.*[19] to propose that slip is modulated by the climate-driven pole-tide, which has period $T \approx 14.3$ months (the pole-tide is a gravitational effect of oscillations in the Earth's rotational axis excited by ocean loading). They modelled plate boundary stress due to the pole-tide and found small (up to ~160 Pa peak-to-peak) stress variations with peak shear at or just after the Puget basin events, and they also qualitatively argue that transitional rate-state rheological conditions favour slip at such long periods.

Slow slip elsewhere recurs at 6- to 18-month intervals, depending on location. Events in Guerrero, Mexico, are quasi-periodic with a 12.0 ± 0.3 month period[9] (Fig. 1). In addition to the 14.7-month Puget basin behaviour, Cascadia events recur at 10.9 ± 1.2 months in northern California[5] and at 14 months in the Explorer plate region, where slip is ~6 months out of phase with Puget activity[6]. Events in the Shikoku region of Japan occur once every six months with alternating initiation locations and directions of propagation[2], suggesting annual periodicity with a 6-month phase difference at either end of the segment.

The ubiquity of quasi-periodic behaviour suggests that cyclical processes at 6–18-month periods somehow induce fault slip. In this Letter, I examine 12-month periodic slow slip in Guerrero, and propose fault system resonance as a quantitative mechanism for amplification of slip response to small cyclical stress perturbations. The Earth's response to loading by climatic redistribution of the atmosphere, hydrosphere and cryosphere is an obvious candidate for inducing stress at periods corresponding to slow slip. From equations for conservation of momentum, Poisson's equation, elasticity and boundary conditions used to calculate load Love numbers[20], I derive expressions applicable everywhere in the Earth's interior for the six independent stress tensor components generated by surface loading (provided as Supplementary Information). Figure 2a depicts an example history of stress at a point on the subduction thrust beneath GPS station COYU. Fault shear and normal stress are shown for the period 1995–2005, assuming a continental PREM[21] Earth model and a Climate Prediction Center model of global surface hydrologic mass[22]. The latter was chosen because continental hydrology dominates global deformation at the annual period[23] that is the focus here. Also shown in Fig. 2b are peak-to-peak shear stress changes everywhere on the plate interface during the same period.

These calculations demonstrate several important features of environmental stress on the plate interface. First, shear and normal stress in Fig. 2a are in phase, and although a few of the Guerrero slip events nearly coincide with peak shear, peak slip-rate follows peak stress by 2.9 ± 1.5 months. The phase of hydrologic load stress

[1]Department of Physics, University of Colorado, Boulder, Colorado 80309-0390, USA. †Present address: Department of Geology, Utah State University, Logan, Utah 84322, USA.

depends on location, but phase on the Cocos–North America plate interface varies by less than a month. Second, shear stress perturbations on the subduction thrust are largest (and normal stress perturbations smallest) near the coastline, coincident with the base of the seismogenic zone (compare with Fig. 1b, c). The amplitude of the stress change is partly conditioned by orographic focusing of precipitation in the coastal Sierra Madre del Sur and partly by the increase of horizontal stress with depth. However, shear and normal stress are most sensitive to fault dip, and the unusual shallow-steep-shallow dip geometry of the plate interface in Guerrero (Fig. 2b inset) amplifies shear and dampens normal stress on the steeply dipping section.

Hydrologic stress perturbations are a factor of two or more larger than those predicted for the pole-tide[19], but 300 Pa is still a negligible fraction (~0.01%) of the stress drop during large interplate earthquakes on the Cocos–North America plate boundary[24]. Hence, it is necessary to assess whether climate-driven stress is at all significant relative to tectonic stress accumulation on similar timescales. Figure 2c depicts the tectonic shear stress accumulation rate in Guerrero (described further in Methods). Peak-to-peak hydrologic stress (Fig. 2b) ranges from ~1% of annual tectonic accumulation (Fig. 2c) near the trench to 5–20% at the base of the seismogenic zone, and can exceed tectonic rates at greater depths where the latter drops near zero.

Frictional slip initiates when shear stress τ exceeds $\mu_f\sigma_e$, where μ_f is the coefficient of static friction and $\sigma_e = \sigma_n - P_f$ is effective normal stress, σ_n is true normal stress and P_f is pore fluid pressure. If μ_f is invariant and stress has a small ratio of annual to secular variation like that estimated for southern Mexico, it is difficult to imagine how this physical formalism could organize slip that is quasi-periodic and has the phase properties observed in Fig. 2a. Hence, for fault slip to be forced by environmental stress, one requires (1) that slip must respond more robustly to stress at periods of about one year than to secular stress or stress at other periods, and (2) that the phase of peak slip can shift significantly from that of peak stress.

Slider-block models of slip, given a rate- and state-dependent friction law[25,26], suggest a mechanism by which both of these conditions may be met. Rate- and state-dependent friction varies, for example, as the Dieterich law[27], $\mu_f = \mu_0 + a\ln(V/V^\star) + b\ln(V^\star\Theta/D_c)$, in which μ_0, a, b and D_c are experimentally determined material constants, V is slip velocity, $V^\star$ is a normalizing velocity and Θ is a time-dependent state variable. Perfettini *et al.*[25] find that slip response to a given stress can amplify dramatically within a narrow band of resonant periods, provided that frictional conditions are velocity-weakening (as defined by $b - a > 0$) and slip is stabilized by the fault's elastic stiffness $k = \dot{\tau}/\dot{u} > k_c$, where u is slip deficit and

$$k_c = \frac{\sigma_n(b-a)}{D_c} \quad (1)$$

is a critical stiffness below which slip destabilizes. In that case, excitation by stress at period T with shear stress amplitude and normal stress amplitude $\tilde{\tau}$ and $\tilde{\sigma}_n$, respectively, perturbs the slip velocity by an amount approximated by[26]:

$$\tilde{V} = qV_{rpm}\frac{q[\tilde{\sigma}_n(\mu_{ss}-\alpha)-\tilde{\tau}] - i(\tilde{\sigma}_n\mu_{ss}-\tilde{\tau})}{kD_c - a\sigma_n q^2 + iqD_c(k-k_c)} \quad (2)$$

in which the dimensionless pulsation $q = 2\pi D_c/TV_{rpm}$, V_{rpm} is relative plate motion velocity, μ_{ss} is steady-state friction and α describes frictional response to a change in normal stress. Slip is unbounded (that is, resonant) when the denominator goes to zero; at critical stiffness ($k = k_c$) this occurs at a critical period:

$$T_c = \frac{2\pi D_c}{V_{rpm}}\sqrt{\frac{a}{b-a}} \quad (3)$$

Fig. 3a depicts an example calculation of perturbational slip velocity $\tilde{V}$ as a function of stiffness k and period T using equation (2). The parameters used (lower-left inset) are consistent with expectations near the base of the seismogenic zone in southern Mexico. Slip response amplifies significantly for a narrow range of periods near T_c when stiffness $k = k_c$, and at shorter periods when $k > k_c$. In addition to stiffness, the resonant period depends on local values

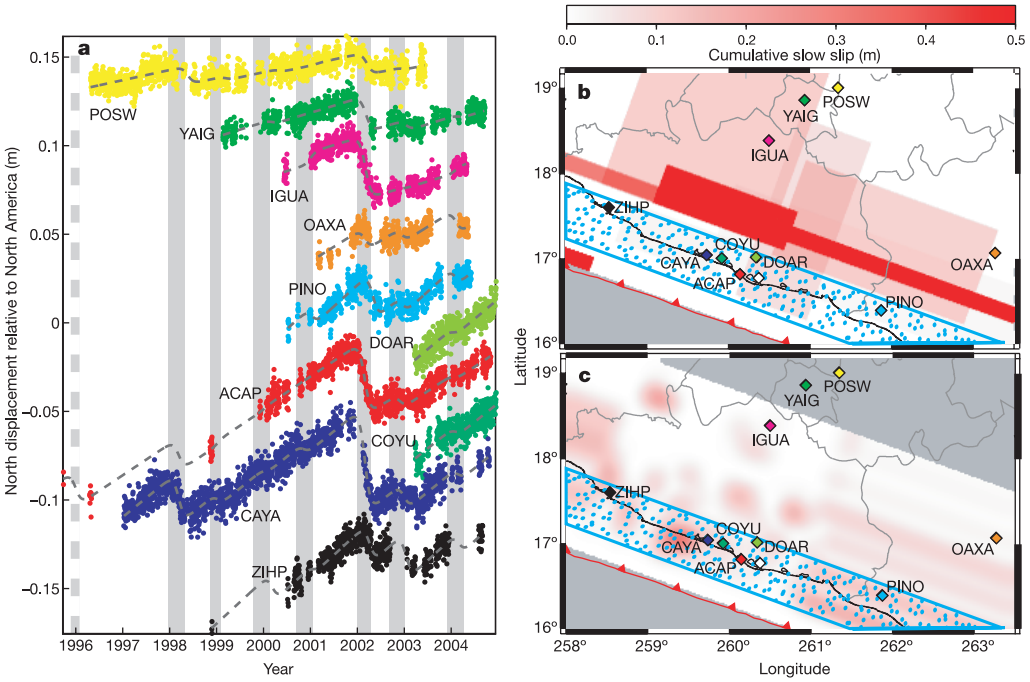

Figure 1 | GPS time series and slow slip models from Guerrero, Mexico. **a**, GPS north positions. Filled circles are daily coordinates, dashed lines are best-fit model[9]. Grey bands indicate timing of slow slip from the GPS data. **b**, **c**, Maps showing locations of GPS sites and surface-projected models of cumulative slow thrust slip[9]: in **b** each event was modelled as uniform slip in a single rectangular patch; in **c** slip was estimated in discretized elements. The stippled blue region approximates the zone of rupture in past great earthquakes.

of a, b, D_c and V_{rpm}. At periods other than the resonant period, slip amplitude is sensitive to assumed model parameters and particularly to $(b - a)$. The very small $(b - a) = 10^{-8}$ assumed in Fig. 3a, likely to occur only near the top and bottom of the seismogenic zone, amplifies slip response to environmental stress by about two orders of magnitude more than would a value of $(b - a) = 10^{-6}$ (Fig. 3a inset). Using $(b - a) = 0.005$, near the laboratory-derived parameter at middle depths of the seismogenic zone[28], reduces response by nearly six orders of magnitude. Hence, slip resonance explains why slow slip should be favoured near the transition from velocity-weakening to velocity-strengthening at the base of the seismogenic zone. Elsewhere in the seismogenic zone, amplification is negligible and/or too narrow-band to excite slip over an area large enough to observe with GPS. In southern Mexico, the largest events slip early on the shallow part of the fault and later on the deeper part[9], suggesting that slip propagates from the seismogenic zone to greater depth, analogous to postseismic slip excited by earthquakes. Dependence of slip amplitude on $(b - a)$ similarly explains why creep events simulated in numerical models focus at the frictional transition[13].

Phase differences between peak stress and peak slip (for example, Fig. 2a) also contain information about resonance properties. Figure 3b shows details of slip velocity amplitude near its maximum for several examples of k/k_c, using the same parameterization as in Fig. 3a. The corresponding dependence of phase is shown in Fig. 3c. In this example, phase γ is zero (that is, slip and stress are in phase) for excitation periods greater than the maximum velocity perturbation, and $\gamma = \pi$ (perfectly out of phase) for periods less than the maximum perturbation. When the resonant period and excitation period coincide, $\gamma = \pi/2$. Phase is somewhat sensitive to parameters assumed in equation (2), but the pattern of $\gamma \approx 0$ on one side of the saddle and $\gamma \approx \pi$ on the other, with transitional phase between, is a persistent feature given small $(b - a)$. Extrapolating to phase relations observed in slow slip events, this implies that the resonant period for the plate boundary in Guerrero is almost exactly one year.

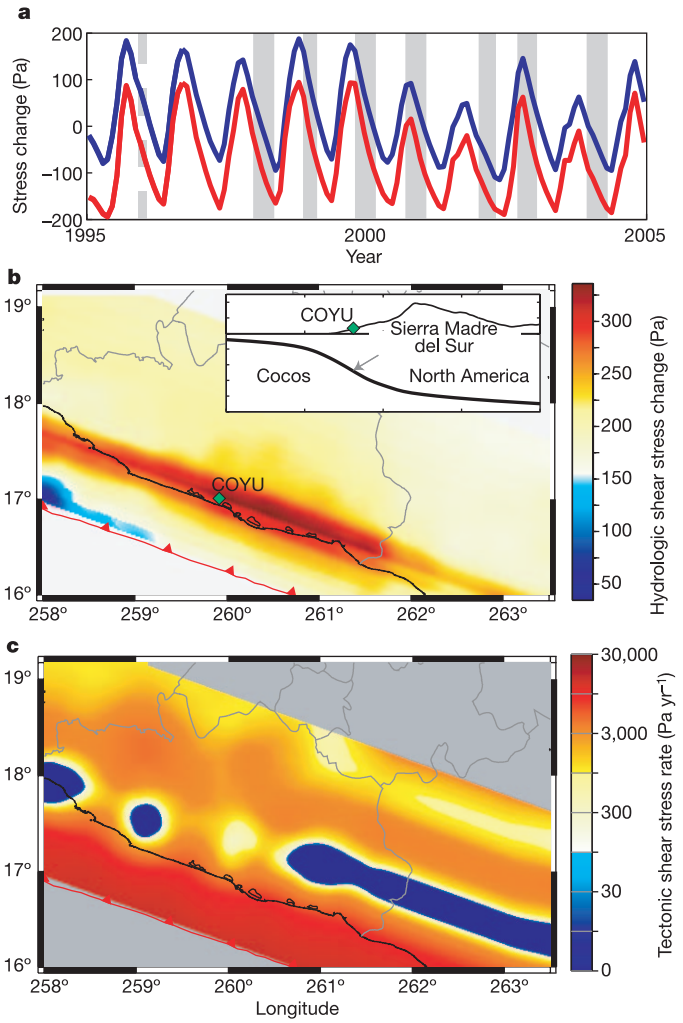

Figure 2 | Stress on the fault surface. **a**, Time series of normal stress (blue; positive indicates fault compression) and shear stress (red; positive favours thrust slip) at a point beneath GPS site COYU. Grey bars denote periods of deep slow slip; peak slip occurs at the centre of the bar. **b**, Map view of peak-to-peak shear stress perturbation, projected from the plate interface to the surface. Inset shows plate geometry and strike-averaged topography versus distance from the trench; arrow indicates location of time series sampled in **a**. **c**, Rate of accumulation of tectonic shear stress.

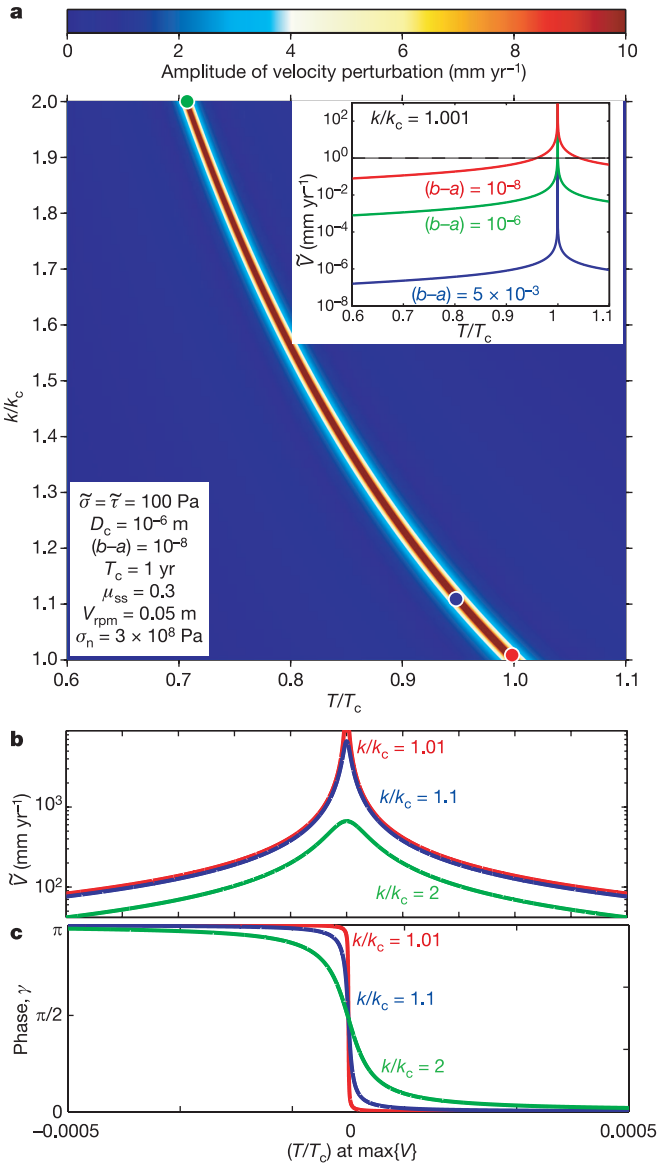

Figure 3 | Relationships of rate- and state-dependent frictional parameters to resonant slow slip. **a**, Slip velocity perturbation as a function of period T and fault stiffness k (normalized to critical values), for frictional parameters shown in lower-left inset (see text for parameter definitions). Upper-right inset, profiles of dependence of velocity amplitude $\tilde{V}$ on T (normalized to critical period, T_c) for alternative values of $(b - a)$. Coloured circles are profiled in detail in **b** and **c**. **b**, Amplitude of slip velocity perturbation near its maximum for $k/k_c = 1.01$ (red), 1.1 (blue) and 2 (green). **c**, Phase of slip (relative peak stress) corresponding to the amplitude profiles shown in **b**.

The Puget basin[4] ($\gamma \approx -\pi/4$) and Explorer plate[6] ($\gamma \approx \pi$) regions of Cascadia apparently resonate at periods slightly offset from (and on opposite sides of) the pole-tide. Similarly, the northeastern ($\gamma \approx 0$) and southwestern ($\gamma \approx \pi$) Shikoku regions[2] may resonate at periods slightly offset from (and on opposite sides of) the annual snow loading cycle in Japan.

Critical stiffness and critical period relations may be useful to infer fault frictional properties. Stiffness $k = \dot{\tau}/\dot{u}$ can be calculated from steady-state slip estimates (for example, using calculations for Fig. 2c). Assuming that Guerrero is near criticality, such that the one-year period $T = T_c$ and $k = k_c$, it is instructive to solve equations (1) and (3) for two unknown frictional parameters a and $(b - a)$ on the fault. Near the base of the Guerrero seismogenic zone, where events most probably initiate, such a calculation yields $a \approx 0.015$ and $(b - a) \approx 10^{-9}$. These values approximate laboratory estimates of frictional parameters at the base of the seismogenic zone[28].

When effects of loading in oceans, atmosphere and tides are included, environmental stress is relatively broad-band with a handful of spectral peaks, so there is a rich spectrum of potential forcing signals for fault slip. Resonant fault slip can be observed geodetically if a large enough patch of the fault can resonate at a single period, or can propagate slip downdip into the velocity-strengthening regime. Fault slip resonance explains why slip events should be periodic, why periods differ from place to place, why the phase of peak slip differs from that of peak environmental stress, and why slip focuses near the base of the seismogenic zone. These events must initiate in velocity-weakening conditions—that is, within the zone of nucleation of a future great earthquake—further suggesting that slow slip events can illuminate the frictional properties that control earthquake slip.

METHODS

To determine the relative contribution of tectonic accumulation versus hydrologic load stress, I estimate the annual rate of change of fault stress due to plate boundary deformation. I first calculate stress induced by fault slip using Green's function relations[29] applied to steady-state virtual slip on the fault. Virtual slip was modelled on a 20 km mesh discretization of the plate boundary using GPS velocities estimated after subtraction of the displacements during slow slip events[9]. The slip-induced stress distribution was smoothed to remove spurious singularities introduced by discontinuous slip at the dislocation boundaries. I then summed the result with stress rates from a two-dimensional elastic finite element model using the far-field (relative plate motion) kinematics as boundary conditions, to correct for the Green's function assumption of zero displacement at infinite distance. The latter turns out to be a negligibly small correction, amounting to a few tens of Pa yr^{-1}. Figure 2c depicts the resulting estimate of shear stress accumulation rate. Tectonic stress accumulation estimated by this approach is qualitatively similar to stress rates estimated directly from finite element modelling of GPS velocities for Cascadia[30]. In both cases, shear stress rates in the seismogenic zone are consistent with measured earthquake stress drops when multiplied by the timescale of the seismic cycle, and rates rapidly drop to small values below the depth of rupture in large interplate earthquakes.

Received 24 October 2005; accepted 3 July 2006.

1. Hirose, H., Hirahara, K., Kimata, F., Fujii, N. & Miyazaki, S. A slow thrust slip event following the two 1996 Hyuganada earthquakes beneath the Bungo Channel, southwest Japan. *Geophys. Res. Lett.* **26,** 3237–3240 (1999).
2. Obara, K., Hirose, H., Yamamizu, F. & Kasahara, K. Episodic slow slip events accompanied by non-volcanic tremors in southwest Japan subduction zone. *Geophys. Res. Lett.* **31**, doi:10.1029/2004GL020848 (2004).
3. Dragert, H., Wang, K. & James, T. S. A silent slip event on the deeper Cascadia subduction interface. *Science* **292,** 1525–1528 (2001).
4. Miller, M. M., Melbourne, T., Johnson, D. J. & Sumner, W. Q. Periodic slow earthquakes from the Cascadia subduction zone. *Science* **295,** 2423 (2002).
5. Szeliga, W., Melbourne, T. I., Miller, M. M. & Santillan, V. M. Southern Cascadia episodic slow earthquakes. *Geophys. Res. Lett.* **31**, doi:10.1029/2004GL020824 (2004).
6. Malone, S., Rogers, G., Dragert, H., McCausland, W. & Johnson, D. Review of Episodic Tremor and Slip in Cascadia. *Eos* **85**, abstr. S53A (2004).
7. Dragert, H., Wang, K. & Rogers, G. Geodetic and seismic signatures of episodic tremor and slip in the northern Cascadia subduction zone. *Earth Planets Space* **56,** 1143–1150 (2004).
8. Lowry, A. R., Larson, K. M., Kostoglodov, V. & Bilham, R. G. Transient slip on the subduction interface in Guerrero, southern Mexico. *Geophys. Res. Lett.* **28,** 3753–3756 (2001).
9. Lowry, A. R., Larson, K. M., Kostoglodov, V. & Sanchez, O. The fault slip budget in Guerrero, southern Mexico. *Geophys. J. Int.* (submitted).
10. Cohen, S. C. & Freymueller, J. T. Crustal deformation in the southcentral Alaska subduction zone. *Adv. Geophys.* **47,** 1–63 (2004).
11. Douglas, A., Beavan, J., Wallace, L. & Townend, J. Slow slip on the northern Hikurangi subduction interface, New Zealand. *Geophys. Res. Lett.* **32**, doi:10.1029/2005GL023607 (2005).
12. Rogers, G. & Dragert, H. Episodic tremor and slip on the Cascadia subduction zone: The chatter of silent slip. *Science* **300,** 1942–1943 (2003).
13. Kao, H. *et al.* A wide depth distribution of seismic tremors along the northern Cascadia margin. *Nature* **436,** 841–844 (2005).
14. Chouet, B. Resonance of a fluid-driven crack: Radiation properties and implications for the source of long-period events and harmonic tremor. *J. Geophys. Res.* **93,** 4375–4400 (1988).
15. Melbourne, T. I. & Webb, F. H. Slow but not quite silent. *Science* **300,** 1886–1887 (2003).
16. Flück, P., Hyndman, R. D. & Wang, K. Three-dimensional dislocation model for great earthquakes of the Cascadia subduction zone. *J. Geophys. Res.* **102,** 20539–20550 (1997).
17. Shibazaki, B. & Iio, Y. On the physical mechanism of silent slip events along the deeper part of the seismogenic zone. *Geophys. Res. Lett.* **30**, doi:10.1029/2003GL017047 (2003).
18. Liu, Y. & Rice, J. R. Aseismic slip transients emerge spontaneously in three-dimensional rate and state modeling of subduction earthquake sequences. *J. Geophys. Res.* **110**, doi:10.1029/2004JB003424 (2005).
19. Shen, Z. K., Wang, Q., Bürgmann, R. & Wan, Y. Pole-tide modulation of slow slip events at circum-Pacific subduction zones. *Bull. Seismol. Soc. Am.* **95,** 2009–2015 (2005).
20. Wahr, J. M. in *Geodesy and Global Geodynamics* (eds Moritz, H. & Sunkel, H.) 327–380 (Technical University of Graz, Austria, 1983).
21. Dziewonski, A. M. & Anderson, D. L. Preliminary reference Earth model. *Phys. Earth Planet. Inter* **25,** 297–356 (1981).
22. Fan, Y. & van den Dool, H. Climate Prediction Center global monthly soil moisture data set at 0.5 degrees resolution for 1948 to present. *J. Geophys. Res.* **109**, doi:10.1029/2004JD004345 (2004).
23. Wahr, J. M., Molenaar, M. & Bryan, F. Time variability of the Earth's gravity field: Hydrological and oceanic effects and their possible detection using GRACE. *J. Geophys. Res.* **103,** 30205–30230 (1998).
24. Anderson, J. G. *et al.* Strong ground motion from the Michoacan, Mexico, earthquake. *Science* **233,** 1043–1049 (1986).
25. Perfettini, H., Schmittbuhl, J., Rice, J. R. & Cocco, M. Frictional response induced by time-dependent fluctuations of the normal loading. *J. Geophys. Res.* **106,** 13455–13472 (2001).
26. Perfettini, H. & Schmittbuhl, J. Periodic loading on a creeping fault: Implications for tides. *Geophys. Res. Lett.* **28,** 435–438 (2001).
27. Dieterich, J. H. Modeling of rock friction 1. Experimental results and constitutive equations. *J. Geophys. Res.* **84,** 2161–2168 (1979).
28. Blanpied, M. L., Lockner, D. A. & Byerlee, J. D. Frictional slip of granite at hydrothermal conditions. *J. Geophys. Res.* **100,** 13045–13064 (1995).
29. Okada, Y. Internal deformation due to shear and tensile faults in a half-space. *Bull. Seismol. Soc. Am.* **82,** 1018–1040 (1992).
30. Williams, C. A. & McCaffrey, R. Stress rates in the central Cascadia subduction zone inferred from an elastic plate model. *Geophys. Res. Lett.* **28,** 2125–2128 (2001).

Supplementary Information is linked to the online version of the paper at www.nature.com/nature.

Acknowledgements I thank K. Larson for analysis of GPS data used in this paper; V. Kostoglodov, O. Sanchez and J.A. Santiago for contributions to instrumentation and data collection in Mexico; and J. Wahr and R. Bilham for discussions about the topic of this paper. This research was supported by the National Science Foundation.

Author Information Reprints and permissions information is available at npg.nature.com/reprintsandpermissions. The author declares no competing financial interests. Correspondence and requests for materials should be addressed to the author (arlowry@himalaya.colorado.edu).